Published in final edited form as:
Phys Med Biol. 2010 March 7; 55(5): 1279–1293. doi:10.1088/0031-9155/55/5/002.

Toward acquiring comprehensive radiosurgery field commissioning data using the PRESAGE®/optical-CT 3D dosimetry system

Corey Clift[1], **Andrew Thomas**[1], **John Adamovics**[2], **Zheng Chang**[1], **Indra Das**[3], and **Mark Oldham**[1]

Corey Clift: cclift@montefiore.org

[1] Department of Radiation Oncology, Duke University Medical Center, Durham, NC 27710, USA

[2] Department of Chemistry, Rider University, Lawrenceville, NJ 08648, USA

[3] Department of Radiation Oncology, Indiana University School of Medicine, Indianapolis, IN 46202, USA

Abstract

Achieving accurate small field dosimetry is challenging. This study investigates the utility of a radiochromic plastic PRESAGE® read with optical-CT for the acquisition of radiosurgery field commissioning data from a Novalis Tx system with a high-definition multileaf collimator (HDMLC). Total scatter factors ($S_{c,\,p}$), beam profiles, and penumbrae were measured for five different radiosurgery fields (5, 10, 20, 30 and 40 mm) using a commercially available optical-CT scanner (OCTOPUS, MGS Research). The percent depth dose (PDD), beam profile and penumbra of the 10 mm field were also measured using a higher resolution in-house prototype CCD-based scanner. Gafchromic EBT® film was used for independent verification. Measurements of $S_{c,\,p}$ made with PRESAGE® and film agreed with mini-ion chamber commissioning data to within 4% for every field (range 0.2–3.6% for PRESAGE®, and 1.6–3.6% for EBT). PDD, beam profile and penumbra measurements made with the two PRESAGE®/optical-CT systems and film showed good agreement with the high-resolution diode commissioning measurements with a competitive resolution (0.5 mm pixels). The in-house prototype optical-CT scanner allowed much finer resolution compared with previous applications of PRESAGE®. The advantages of the PRESAGE® system for small field dosimetry include 3D measurements, negligible volume averaging, directional insensitivity, an absence of beam perturbations, energy and dose rate independence.

1. Introduction

The measurement of high-resolution commissioning data is a critical step enabling accurate dose calculation in radiosurgery treatments. Commissioning measurements are planning system dependent but generally include percent depth dose, total scatter factors (also called output factors) and beam profiles for a range of field sizes and depths (Das *et al* 2008a). A careful consideration of phantom, detector and measurement geometry is required to achieve accurate measurements. Ideally, measurements are made in water with a detector that exhibits negligible energy, dose rate and directional dependence, as well as insignificant volume averaging. Deviating from the ideal can introduce considerable errors for narrow beam geometries lacking lateral charged particle equilibrium (Das *et al* 2008b). Once the field size becomes smaller than the maximum range of the secondary electrons (roughly equal to the depth of maximum dose (Heydarian *et al* 1996)), lateral charged particle equilibrium begins to decrease (Das *et al* 2008b). Other inaccuracies can arise from

penumbral overlap (Das *et al* 2008b), enhanced directional dependence, field perturbations caused by the presence of a detector in the beam path (Heydarian *et al* 1996), and the field size dependence of water to air mean restricted collisional stopping power ratios (Wu *et al* 1993). Various techniques for small field dosimetry have been proposed (Heydarian *et al* 1996, Arakia *et al* 2004, Aaki *et al* 2005, Pappas *et al* 2005, Wilcox and Daskalov 2007, Pantelis *et al* 2008, Babic *et al* 2009). A recent analysis of the available literature by Sauera and Wilbert (2007) found no existing ideal dosimeter or technique for small field commissioning measurements of output factors.

Other authors have investigated several 3D dosimetry techniques for small fields, including polymer gels (Pappas *et al* 2005, 2008, Pantelis *et al* 2008, Moutsatsos *et al* 2009, Wong *et al* 2009), radiochromic ferrous xylenol-orange gels (Calcina *et al* 2007, Babic *et al* 2009), and leuco crystal violet (LCV) micelle gels (Babic *et al* 2009). Babic *et al* (2009) have recently published work involving the measurement of small field beam data using two 3D dosimeters and had good results. However, each of the 3D dosimeters used in the study required inconvenient procedures to achieve acceptable accuracy. The LCV gel/Vista™ system requires a scattered light contamination correction during optical-CT read-out (Babic *et al* 2009). Additionally, ferrous xylenol-orange gels require the delivery of a 'priming dose' and exhibit chemical diffusion effects (Babic *et al* 2009). Some polymer gels may exhibit a high scatter component as well, along with sensitivity to atmospheric oxygen (Oldham and Kim 2004).

This work presents the first application of the PRESAGE®/optical-CT 3D dosimetry system to small field commissioning. The system enables the acquisition of high-resolution 3D data sets that fully characterize a radiation dose distribution. PRESAGE® is a relatively new, easy to implement 3D dosimeter that has been shown to be accurate and reliable in several studies (Guo *et al* 2006a, 2006b, Sakhalkar and Oldham 2008, Sakhalkar *et al* 2009). It has several potential advantages for small field dosimetry, including negligible volume averaging, dependence on energy, dose rate, or directionality (Adamovics and Maryanski 2006, Guo *et al* 2006b). The PRESAGE® material consists of a radiochromic plastic that exhibits a change in optical density (ΔOD/mm) that is linear with the local absorbed dose, and is spatially stable over time (Adamovics and Maryanski 2006). PRESAGE® is well suited for accurate optical-CT scanning. In contrast with most 3D dosimeters, PRESAGE® requires no external container, limiting optical light refraction and reflection at surface boundaries. The absorptive nature of the radiochromic change, the first generation geometry of the OCTOPUS and the use of telecentric optics in the prototype scanner (see section 2.2) avoid the need for scattered light corrections (Guo *et al* 2006b). The large field of view of the OCTOPUS scanner and large dimensions of the dosimeter used in this work enabled the investigation of five radiosurgery fields using one dosimeter.

The challenges associated with achieving accurate dosimetry in small field applications are such that the American Association of Physicists in Medicine has recently commissioned a task group (TG-155 chaired by Das *et al*) to investigate the issues. These challenges, and the lack of established clinical protocol, provide a rationale for our investigation of a technique for the acquisition of small field commissioning data with the aforementioned unique advantages. For commissioning purposes, the PRESAGE®/optical-CT system shows promise by facilitating a rapid acquisition of multiple beam characteristics in one delivery of radiation.

2. Methods

The PRESAGE®/optical-CT system was applied to acquire a subset of the commissioning data for the small radiosurgery fields produced by the Novalis Tx. The delivery system

incorporates an HD-120 MLC that uses 120 leaves; sixty-four 2.5 mm leaves in the center and fifty-six 5 mm toward the outer edges (Chang *et al* 2008). It can be operated in normal 6 MV mode with a maximum nominal dose rate of 600 MU per minute or in SRS mode, which uses a different target and has a nominal dose rate of 1000 MU per minute. The original clinical commissioning output measurements were made with a radiosurgery ion chamber (Ionization Chamber CC01, Wellhofer) with a cavity volume of 0.01 cm^3 and radius of 1.0 mm. Beam profiles and percent depth dose (PDD) curves were measured with a high-resolution diode detector (Hi-pSi stereotactic field detector, Scanditronix) with a sensitive volume 0.6 mm in diameter and 0.6 mm thick. These measurements have been described in Chang *et al* (2008). The small field commissioning data required by the planning system consisted of square fields with nominal side lengths of 40, 30, 20, 10 and 5 mm. Although the fields were defined by the HDMLC, the jaws were set to a square field size that is 2 mm larger than the MLC field.

Two optical-CT scanners were used in this study. The first was a commercial system (OCTOPUS, MGS Research) which had a large field of view (25 cm), and was used to acquire total scatter factors ($S_{c,\,p}$) and profile data in a large PRESAGE® dosimeter irradiated with multiple radiosurgery fields. The second was an in-house prototype scanner with a small field of view (6 cm), but much higher spatial resolution (~0.05 mm), which was used to measure the PDD and profile data in a small PRESAGE® dosimeter. This scanner is a development of that presented in Sakhalkar and Oldham (2008), and represents an improvement on earlier designs (Wolodzko *et al* 1999, Doran *et al* 2001), as it incorporates tertiary scatter rejecting telecentric imaging optics. In principle, all measurements could have been made with a single dosimeter and a larger version of the prototype scanner. In practice this was not achievable due to the current limited field of view of the prototype. Gafchromic EBT® film was used as an independent verification of all PRESAGE® measurements and direct comparisons were made between experimental dosimetry and established commissioned values of percent depth dose, beam penumbra and $S_{c,\,p}$. Table 1 summarizes the measurements made during this study.

2.1. PRESAGE® dosimeters

A large cylindrical PRESAGE® dosimeter (height of 11 cm, a diameter of 16 cm) was used to determine output factors for all beams, irradiated in the geometry shown in figure 1(a). The dosimeter had a CT number of 210 ± 5.5 HU and a mass density of 1.05 g cm^{-3}. A small dosimeter was used to determine PDD and beam profiles and was irradiated with a single field incident on the flat top of the cylinder, centered on the middle of the dosimeter. The small dosimeter was cylindrical in shape with a height of 53 mm, a diameter of 60 mm, a CT number of 172 ± 4.8 HU and a mass density of 1.05 g cm^{-3}. Both dosimeters were accompanied by optical cuvettes containing PRESAGE® from the same batch. The cuvettes were irradiated at different dose levels to determine sensitivity and confirm the expected and well-established linear relationship between ΔOD/mm and the calculated absorbed dose reported in other work (Guo *et al* 2006a, 2006b, Sakhalkar and Oldham 2008, Sakhalkar *et al* 2009). The linear response of the larger volumes was assumed. The validation of this assumption and the potential of using cuvette data as a means of calibration is a topic of future study.

2.2. Optical-CT scanning

The large PRESAGE® dosimeter was scanned with the OCTOPUS laser-based optical-CT scanner. This scanner transmits a He–Ne laser beam through the rotating sample in one plane and then steps the laser through the sample vertically to acquire data from different slices. The sample is housed in an aquarium containing optical refractive index matching fluid to limit the refraction of light passing through the sample preserving the parallel ray

geometry. The slice thickness and in-plane resolution are defined by the width of the laser beam. This scanner has been described in other works (Islam *et al* 2003, Doran and Krstajić 2006, Guo *et al* 2006a). In order to measure ΔOD/mm within the dosimeter, an optical-CT scan was performed before and after irradiation. Both scans consisted of 1200 projections through 360°, meeting the Nyquist angular sampling criterion (Webb 1988). The following filtered back projection reconstruction resulted in one slice at a depth of 5 cm from the surface of the dosimeter with 0.5 × 0.5 × 0.5 mm voxels. The pre- and post-irradiation slices were then registered manually and subtracted in order to obtain an image consisting ΔOD for corresponding voxels.

The small dosimeter was scanned using the prototype CCD-based scanner first described by Sakhalkar and Oldham (2008). It makes use of a diffuse backlight and a CCD camera with a telecentric lens. The collimation of visible light is made possible by the telecentric lens. The lens only accepts incoming light within 0.2° of its central axis. An additional characteristic is the lack of magnification changes with object distance changes shown by telecentric lenses. The sample, as shown in figure 2, is housed in an aquarium filled with optical refractive index matching fluid (again, to preserve the parallel ray geometry) and rests on a rotation stage fixed to a stepper motor to control sample rotation. At any given orientation this type of optical-CT device allows for the acquisition of many slices at once without scanning a light source laterally and vertically. This reduces the time needed to complete a scan from 1–24 h (depending on sample size) as with the OCTOPUS to 1–20 min (depending on sample size). There is also an advantage of an order of magnitude finer resolution. The detector used with the prototype scanner is a 12-bit 1040 × 1392 pixel CCD camera. The camera is attached to a telecentric lens with a magnification factor of 1/8. The physical pixel size is 6.45 μm^2 resulting in image pixels measuring 51.6 μm^2. The combination of this particular CCD and telecentric lens limits the field of view to a height of 54 mm and a width of 72 mm. In order to measure ΔOD/mm within the dosimeter, an optical-CT scan was performed before and after irradiation using the CCD-based scanner. Both scans consisted of 360 projections through 180°. The angular sampling rate was roughly half of that used with the OCTOPUS because fewer projections were needed to meet the Nyquist sample criterion. The following reconstruction resulted in a 3D digitization of the entire dosimeter. In order to speed up data reconstruction time, reduce the total data stored in memory and decrease noise, each projection image was resampled bilinearly from the original 51.6 μm pixel size. The result was a projection image set with 238 μm square pixels and reconstructed pre- and post-irradiation data cubes with 238 × 238 × 238 μm voxels. The pre- and post-irradiation volumes were then registered manually and subtracted in order to obtain a data cube consisting of the ΔOD/mm for each voxel. In order to reduce noise and ring artifacts, two images per angular orientation were taken and averaged. Both the dark field and flood field correction images were obtained by averaging 300 exposures. Reconstruction was accomplished using commercially available software called Cobra (Exxim Corp) which implements a Feldkamp algorithm designed to quickly reconstruct volumes of tomographic data.

2.3. EBT film methods

EBT film is well suited for radiosurgery applications because it shows good tissue equivalence, little dose rate dependence, fine resolution, exhibits a stable radiochromic response, is adaptable for insertion into various phantoms and is insensitive to room light (McLaughlin *et al* 1994, Wilcox and Daskalov 2007, Wong *et al* 2009). All optical absorbance measurements in this study were carried out using an Epson 4990 flat bed transmission scanner with pixel size of 84.5 μm. In order to measure ΔOD, three scans of each film were performed before and after irradiation. Averaging three consecutive scans has been shown to increase the accuracy of EBT-based dosimetry (Martisikova *et al* 2008).

The values in the averaged pre- and post-irradiation arrays were converted to optical density, registered and subtracted pixel-wise to measure ΔOD.

EBT film exhibits a nonlinear relationship between ΔOD per Gy absorbed, which necessitates a calibration procedure. Two calibration films from the same batch were acquired consisting of five 4 cm square fields each. The delivered fields deposited a range of 0.54 Gy to 7.84 Gy as calculated by Eclipse and confirmed with ion chamber measurements. ΔOD for each irradiated area was then plotted against the dose as measured with an ion chamber and fitted to a polynomial. This provided a calibration expression to use in transforming ΔOD pixel values from other films in the same batch to absorbed dose values. Two films were used during calibration in order to maximize the spatial separation of the ten fields delivered.

2.4. Total scatter factor measurements

$S_{c,\,p}$ is defined as the ratio $D(r, d_{\mathrm{ref}})/D(r_{\mathrm{ref}}, d_{\mathrm{ref}})$, where $D(r_{\mathrm{ref}}, d_{\mathrm{ref}})$ is the absorbed dose per monitor unit to a point in water at a depth of d_{ref} for a field size r. $D(r, d_{\mathrm{ref}})$ is the dose absorbed per monitor unit to a point at a depth of d_{ref} for a field size r_{ref}. This ratio is defined for a point on the central axis and is independent of dose rate. Typically the SSD is 100 cm, the reference depth is the depth of maximum dose, and the reference field size is 10 cm × 10 cm. The original commissioning data for the Novalis Tx include total scatter factor measurements for 40, 20, 10 and 5 mm fields with an SSD of 100 cm at a depth of 5 cm. These measurements were made with a Wellhofer CC01 compact ion chamber and water tank.

With a source to surface distance of 100 cm, the large PRESAGE® dosimeter was irradiated with 845 MU per field in SRS mode in the arrangement shown in figure 1(a). This number of monitor units corresponded to the deposition of 8.45 Gy under calibration conditions. A 5 mm field (top right and bottom left in figure 1(a)) was delivered in two locations so that in the event of one field being obscured by a flaw in the dosimeter, a determination of $S_{c,\,p}$ would not be hindered. The output factors relative to the 40 mm field (OF_{40}) for each field size r were calculated using the equation

$$OF_{40}(r)=D(r, d_{\mathrm{ref}})/D(40, d_{\mathrm{ref}}). \tag{1}$$

The total scatter factor for each field size relative to a 100 mm field size was calculated using

$$S_{c,p}(r)=OF_{40}(r)\times S_{c,p}(40), \tag{2}$$

where $S_{c,\,p}(40)$ is the total scatter factor for a 40 mm field as measured during the initial commissioning. The inter-field dose contamination resulting from the irradiation geometry in figure 1(a) was investigated with EBT film as discussed subsequently.

Following from equations (1) and (2), and the linear relationship between ΔOD and deposited dose, $S_{c,\,p}$ was initially calculated from the optical-CT scan for each field using

$$S_{c,p}(r)=OF_{40}(r)\times S_{c,p}(40)=\frac{\Delta\mathrm{OD}(r, d_{\mathrm{ref}})}{\Delta\mathrm{OD}(40, d_{\mathrm{ref}})}\times S_{c,p}(40). \tag{3}$$

The value of $\Delta OD(r, d_{ref})$ was determined by averaging the value of the voxels in a circular region of interest centered on each field of size r in the reconstructed subtraction slice located at a d_{ref} of 5 cm. Averaging multiple voxels was favored over using the smallest possible ROI (one voxel) in order to reduce the uncertainty resulting from noise in the data. To limit the ROI sampling error associated with averaging multiple voxels, a zero volume measurement was estimated by an extrapolation from measurements made with gradually decreasing ROI sizes. Pappas *et al* (2005) have shown this has an effect similar to that of varying the sensitive volume of a point detector. Additionally, the total scatter factor for each field was independently determined with EBT film. One piece of EBT film was irradiated with radiosurgery fields in the geometry shown in figure 1(a). Each field was also delivered to separate films individually. These results were later compared to characterize the inter-field dose contamination resulting from the irradiation geometry in figure 1(a). Each film was placed between solid water phantoms at a depth of 5 cm and an SSD of 100 cm and irradiated with 309 MU per field. A circular ROI in the center of each field in the calibrated arrays was used for scatter factor determination. The diameter of each ROI was 5% of the nominal field size. The dose per monitor unit was determined by taking the median pixel value in the ROI in the calibrated arrays. The uncertainty in one pixel was determined by computing the standard deviation in the pixel values within the ROI in the 40 mm field.

2.5. Percent depth dose measurements

With an SSD of 100 cm, a 10 mm square field was delivered in normal mode (6 MV at 600 MU min^{-1}) along the central axis of the small PRESAGE® dosimeter. This resulted in the deposition of a maximum of 8 Gy, which was determined by preliminary cuvette data to be optimal for contrast during optical-CT scanning. The average value of ΔOD/mm within a 1 mm square ROI taken in each slice, normalized by the value at the depth of maximum dose, was used to calculate PDD. This ROI was of a sufficiently small size in order to avoid the systematic errors discussed for measuring $S_{c,\,p}$ (Bjarngard *et al* 1990, Das *et al* 2000). Although the small PRESAGE® dosimeter could have physically accommodated more fields or a single larger field, one 10 mm field was chosen as a simple application that would illustrate the advantages of the prototype scanner. A measurement of PDD could have been made with the OCTOPUS scanner. This would have allowed for measurements far deeper than those made with the CCD-based scanner. However, the slow scan speed and courser out of plane resolution rendered this impractical.

An independent measurement was performed using one piece of EBT film sandwiched vertically between two 5 cm thick pieces of solid water. The film and solid water construction was aligned, edge-on, with the central axis of the beam. 200 MU were delivered in normal mode (600 MU min^{-1}) with a 10 mm field. The resulting data array was resampled bilinearly by a factor that resulted in 1.0 mm square pixels. The percent depth dose was calculated by normalizing the pixel values along the central axis by the pixel value at a depth of 1.4 cm.

2.6. Beam profile and penumbra measurements

The PRESAGE® data volumes previously discussed were further analyzed for beam profile and penumbra measurements. The profiles and penumbrae measured in all fields with the large PRESAGE® dosimeter were compared to diode commissioning measurements made at a depth of 5 cm. The beam profile and penumbra of the 10 mm field was also measured with the small PRESAGE® dosimeter and compared to both the commissioning data and the large PRESAGE® dosimeter data. EBT film has been shown to be accurate in measuring beam penumbra (Cheung *et al* 2006). The EBT film data array, obtained using methods

discussed in sections 2.3 and 2.4, was resampled to yield 0.2 mm square pixels. After this resizing to reduce noise, the array was used to measure the penumbra widths independently.

3. Results and discussion

3.1. Total scatter factors

Table 3 shows a comparison of both the experimentally determined and the commissioning values of $S_{c,\,p}$. The reconstructed subtraction slice from the large PRESAGE® dosimeter located at a depth of 5 cm is shown in figure 1(b). A three-dimensional surface rendering of the entire volume is shown in figure 1(c). The standard deviation in the average pixel values used for $S_{c,\,p}$ measurements was 2.5%. A recent and rigorous analysis of the accuracy and reproducibility of PRESAGE® shows a percent uncertainty of 3% including potential sources of systematic error including intra-dosimeter nonuniformity, inter-dosimeter differences and dosimeter ageing characteristics (Sakhalkar *et al* 2009). This conservative value was adopted over the 2.5% statistical error found here because this work did not examine, and inevitably ignores, such a wide range of potential sources of error. Optical cuvette experiments confirmed the linearity of dose response with a coefficient of determination of 0.998. This strongly suggests that the cylindrical volume of PRESAGE® will have a linear response at similar dose levels and that the sensitivity (ΔOD/Gy) will be similar though this has not been rigorously verified at this point.

The measurement of $S_{c,\,p}$ for the 5 mm field showed the largest percent difference (3.6%) with respect to the commissioning data. The predominant sources or error in the data included debris small enough to pass through the filtration system suspended in the refractive index matching fluid used for optical-CT scanning and flaws within the dosimeter causing local intra-dosimeter response nonuniformity (shown by Sakhalkar *et al* (2009) to be within 2%). Additional optical flaws exist in the form of debris and small bubbles suspended in the PRESAGE® matrix. Another source of error present in every field measurement arises from the departure from water equivalence exhibited by PRESAGE®. This may have slightly increased the lateral electronic equilibrium and affected the measured scatter factors. Such effects have been reported in the literature (Tello *et al* 1995). It is likely that such sources of error, including nonuniformity, optical flaws and water inequivalence will be minimized with improved dosimeter manufacturing procedures and the development of more water equivalent formulas.

The EBT measured values of $S_{c,\,p}$ were computed from data acquired on separate films with individual fields in order to exclude possible inter-field dose contamination. A statistical percent uncertainty of less than 1% was calculated for each measured value. However, in order to reflect potential systematic forms error, the 2σ dose uncertainty calculated in a recent and thorough analysis (Saur and Frengen 2008) of EBT dosimetry was adopted (6%). Other authors have shown techniques to increase the precision of dose measurements made with EBT by correcting for the light scattering characteristics of the film (Saur and Frengen 2008, Miras and Arrans 2009). The data in table 2 reflect the effect of inter-field dose contamination present in the irradiation geometry shown in figure 1(a). These data were used to calculate a simple correction for the contamination dose in the PRESAGE® data. This correction consisted of scaling the PRESAGE® measurements by the ratio of the combined and separate geometry measurements in table 2. The resulting corrected values are reported in table 3. This small effect is due to phantom scatter and leakage radiation and could be minimized by using a larger dosimeter with greater field spacing, fewer fields, or more effective collimation.

3.2. Percent depth dose

Figure 3(a) shows an example projection from the post irradiation projection set. It is one of 360 projection images acquired during the scan. The linearity of the visible radiochromic change with respect to dose within this dosimeter was confirmed by optical cuvette experiments resulting in a coefficient of determination of 0.999. The implications of this are discussed in section 3.1. A slice through the subtraction volume is shown in figure 3(b). Figure 4(a) shows the PDD curve determined with PRESAGE®, and with EBT film. Both curves were normalized by the dose absorbed at a depth of 14 mm.

The measurements of PDD presented here exhibit good agreement with established methods of dosimetry but carry more noise. As with the OCTOPUS, the predominant sources or error include debris suspended in the refractive index matching fluid, intra-dosimeter response nonuniformity and optical flaws within the dosimeter. Debris in the fluid and within the dosimeter was of less concern using the OCTOPUS due to its courser resolution. This nonstatistical noise is visible in figures 3(a) and (b). Areas with reconstruction artifacts, such as rings, produce noisy areas in the PDD data with deviations that are not present in the other artifact free areas. These rings are common reconstruction artifacts that usually result from inadequate or incorrect flood corrections (Doran and Krstajić 2006). In order to limit ring artifacts, any feature apart from the dosimeter present in every projection must be eliminated (Doran and Krstajić 2006). These features include but are not limited to debris small enough to pass through the filtration systems suspended in the fluid. Upon removing the dosimeter from the scanner to acquire a flood (also known as flat) image, the suspended debris inevitably moved to a different location in the field of view. This made it impossible to eliminate features resulting from suspended debris through a basic flood correction. As a result, using well-filtered refractive index matching fluid, free of this debris, is the most important factor in reducing these artifacts.

3.3. Beam profile and penumbra

Figure 5(a) shows the profile at 5 cm depth of a 10 × 10 mm field measured with EBT film, the PRESAGE®/CCD optical-CT system and the PRESAGE®/OCTOPUS optical-CT system. Figure 6 shows the profiles measured with EBT and with the large PRESAGE® dosimeter for the remaining fields. The experimental profiles showed good agreement with the commissioning data. A quantitative assessment of the 80–20% penumbrae is shown in table 4. Due to its comprehensive nature, all profiles and penumbrae at depths between 0 and 50 mm in any direction are contained in the data set. A proposed larger scanner could accommodate a greater range of depth.

The data show that much like EBT film, PRESAGE® dosimetry is well suited to make profile measurements required during commissioning. The disparity in resolution between the OCTOPUS and the CCD-based optical-CT scanner did not prove to be of much consequence apart from the differences in uncertainty in the measured penumbra. Other authors have shown a sharper measured penumbra when using EBT compared to 3D techniques (Wong *et al* 2009). The results of this work also show sharper penumbrae measured with EBT, however all experimental measurements of the penumbrae agreed with the commissioning measurements within the experimental uncertainty.

4. Conclusion

The process of commissioning small fields is known to be error prone and resource intensive. The PRESAGE®/optical-CT 3D dosimetry system shows potential as a new approach toward efficiently measuring the commissioning data of radiosurgery fields. This work shows that in its current state of development, an accuracy of measured output within

4% with respect to the currently accepted commissioning technique is achievable with the PRESAGE®/optical-CT system. It enables the measurement of $S_{c,p}$, PDD, and beam profiles with negligible directional, energy, and dose rate dependence all in a truly comprehensive and 3D manner. Being both a dosimeter and a phantom, the beam perturbations and placement errors that occur with a water tank and point detector system are almost absent. In addition, the problem of choosing a dosimeter with an appropriate sensitive volume is avoided by the inherent fine resolution of the optical-CT technique. In the future, reaching the goal of a more water equivalent formulation of PRESAGE® will increase accuracy. Additionally, PRESAGE® dosimetry will benefit from larger CCD-based optical-CT scanners. Using larger telecentric lenses and larger light sources would combine the large field of view associated with the OCTOPUS and the speed and resolution of the prototype CCD-based scanner. Such a scanner would enable all of the measurements shown in this work to be made at deeper depths, with larger fields, in high-resolution 3D, with one dosimeter, one exposure and one optical-CT scan.

Acknowledgments

This research was supported by NIH grant RO1CA100835.

References

Aaki F, Ishidoya T, Ikegami T, Moribe N, Yamashita Y. Application of a radiophotoluminescent glass plate dosimeter for small field dosimetry. Med Phys 2005;32:1548–54. [PubMed: 16013713]

Adamovics J, Maryanski MJ. Characterisation of PRESAGE® : a new 3-D radiochromic solid polymer dosemeter for ionising radiation. Radiat Prot Dosim 2006;120:107–12.

Arakia F, Moribe N, Shimonobou T, Yamashita Y. Dosimetric properties of radiophotoluminescent glass rod detector in high-energy photon beams from a linear accelerator and cyber-knife. Med Phys 2004;31:1980–6. [PubMed: 15305450]

Babic S, McNiven A, Battista J, Jordan K. Three-dimensional dosimetry of small megavoltage radiation fields using radiochromic gels and optical CT scanning. Phys Med Biol 2009;54:2463–81. [PubMed: 19336848]

Bjarngard BE, Tsai JS, Rice RK. Doses on the central axes of narrow 6-MV x-ray beams. Med Phys 1990;17:794–9. [PubMed: 2122197]

Calcina CSG, de Oliveira LN, de Almeida C, de Almeida A. Dosimetric parameters for small field sizes using Fricke xylenol gel, thermoluminescent and film dosimeters, and an ionization chamber. Phys Med Biol 2007;52:1431–9. [PubMed: 17301463]

Chang Z, Wang Z, Wu Q, Yan H, Bowsher J, Zhang J, Yin FF. Dosimetric characteristics of Novalis Tx system with high definition multileaf collimator. Med Phys 2008;35:4460–3. [PubMed: 18975693]

Cheung T, Butson MJ, Yu PK. Measurement of high energy x-ray beam penumbra with Gafchromic EBT® radiochromic film. Med Phys 2006;33:2912–4. [PubMed: 16964868]

Das IJ, Cheng CW, Watts RJ, Ahnesjo A, Gibbons J, Li XA, Lowenstein J, Mitra RK, Simon WE, Zhu TC. Accelerator beam data commissioning equipment and procedures: report of the TG-106 of the Therapy Physics Committee of the AAPM. Med Phys 2008a;35:4186–215. [PubMed: 18841871]

Das IJ, Ding GX, Ahnesjo A. Small fields: nonequilibrium radiation dosimetry. Med Phys 2008b; 35:206–15. [PubMed: 18293576]

Das IJ, Downes MB, Kassaee A, Tochner Z. Choice of radiation detector in dosimetry of stereotactic radiosurgery–radiotherapy. J Radiosurgery 2000;3:177–86.

Das, et al. Task Group No. 155: Small Fields and Non-Equilibrium Condition Photon Beam Dosimetry. unpublished. Doran SJ, Koerkamp KK, Bero MA, Jenneson P, Morton EJ, Gilboy WB. A CCD-based optical CT scanner for high-resolution 3-D imaging of radiation dose distributions: equipment specifications, optical simulations and preliminary results. Phys Med Biol 2001;4:3191–213. [PubMed: 11768500]

Doran SJ, Krstajić N. The history and principles of optical computed tomography for scanning 3-D radiation dosimeters. J Phys Conf Ser 2006;56:45–57.

Guo P, Adamovics J, Oldham M. A practical three-dimensional dosimetry system for radiation therapy. Med Phys 2006a;33:3962–72. [PubMed: 17089858]

Guo PY, Adamovics JA, Oldham M. Characterization of a new radiochromic three-dimensional dosimeter. Med Phys 2006b;33:1338–45. [PubMed: 16752569]

Heydarian M, Hoban PW, Beddoe. A comparison of dosimetry techniques in stereotactic radiosurgery. Phys Med Biol 1996;41:93–110. [PubMed: 8685261]

Islam KT, Dempsey JF, Ranade MK, Maryanski MJ, Low DA. Initial evaluation of commercial optical CT-based 3-D gel dosimeter. Med Phys 2003;30:2159–68. [PubMed: 12945982]

Martisikova M, Ackermann B, Jakel O. Analysis of uncertainties in Gafchromic EBT® film dosimetry of photon beams. Phys Med Biol 2008;53:7013–27. [PubMed: 19015581]

McLaughlin WL, Soares CG, Sayeg JA, McCullough EC, Kline RW, Wu A, Maitz AH. The use of a radiochromic detector for the determination of stereotactic radiosurgery dose characteristics. Med Phys 1994;21:379–88. [PubMed: 8208212]

Miras H, Arrans R. An easy method to account for light scattering dose dependence in radiochromic films. Med Phys 2009;36:3866–9. [PubMed: 19810458]

Moutsatsos A, Petrokokkinos L, Zourari K, Papagiannis P, Karaiskos P, Dardoufas K, Damilakis J, Seimenis I, Georgiou E. Gamma Knife relative dosimetry using VIP polymer gel and EBT radiochromic films. J Phys Conf Ser 2009;164:012053.

Oldham M, Kim L. Optical-CT gel-dosimetry II: optical artifacts and geometrical distortion. Med Phys 2004;31:1–11. [PubMed: 14761013]

Pantelis E, Antypas C, Petrokokkinos L, Karaiskos P, Papagiannis P, Kozicki M, Georgiou E, Sakelliou L, Seimenis I. Dosimetric characterization of CyberKnife radiosurgical photon beams using polymer gels. Med Phys 2008;35:2312–20. [PubMed: 18649464]

Pappas E, Maris TG, Zacharopoulou F, Papadakis A, Manolopoulos S, Green S, Wojnecki C. Small SRS photon field profile dosimetry performed using a PinPoint air ion chamber, a diamond detector, a novel silicon-diode array (DOSI), and polymer gel dosimetry. Analysis and intercomparison. Med Phys 2008;35:4640–8. [PubMed: 18975710]

Pappas E, Petrokokkinos L, Angelopoulos A. Relative output factor measurements of a 5 mm diameter radiosurgical photon beam using polymer gel dosimetry. Med Phys 2005;32:1513–20. [PubMed: 16013707]

Sakhalkar HS, Adamovics J, Ibbott G, Oldham M. A comprehensive evaluation of the PRESAGE®/optical-CT 3-D dosimetry system. Med Phys 2009;36:71–82. [PubMed: 19235375]

Sakhalkar HS, Oldham M. Fast, high-resolution 3-D dosimetry utilizing a novel optical-CT scanner incorporating tertiary telecentric collimation. Med Phys 2008;35:101–11. [PubMed: 18293567]

Sauera O, Wilbert J. Measurement of output factors for small photon beams. Med Phys 2007;34:1983–8. [PubMed: 17654901]

Saur S, Frengen J. GafChromic EBT film dosimetry with flatbed CCD scanner: a novel background correction method and full dose uncertainty analysis. Med Phys 2008;35:3094–101. [PubMed: 18697534]

Tello VM, Tailor RC, Hanson WF. How water equivalent are water-equivalent solid materials for output calibration of photon and electron beams. Med Phys 1995;22:1177–89. [PubMed: 7565393]

Webb, S. The Physics of Medical Imaging. Bristol: Hilger; 1988.

Wilcox EE, Daskalov GM. Evaluation of Gafchromic EBT® film for Cyberknife dosimetry. Med Phys 2007;34:1967–74. [PubMed: 17654899]

Wolodzko JG, Marsden C, Appleby A. CCD imaging for optical tomography of gel radiation dosimeters. Med Phys 1999;26:2508–13. [PubMed: 10587241]

Wong CJ, Ackerly T, He C, Patterson W, Powell CE, Qiao G, Solomon DH, Meder R, Geso M. Small field size dose-profile measurements using gel dosimeters, gafchromic films and micro-thermoluminescent dosimeters. Radiat Meas 2009;44:249–56.

Wu A, Zwicker RD, Kalend AM, Zheng Z. Comments on dose measurements for a narrow beam in radiosurgery. Med Phys 1993;20:777–9. [PubMed: 8350836]

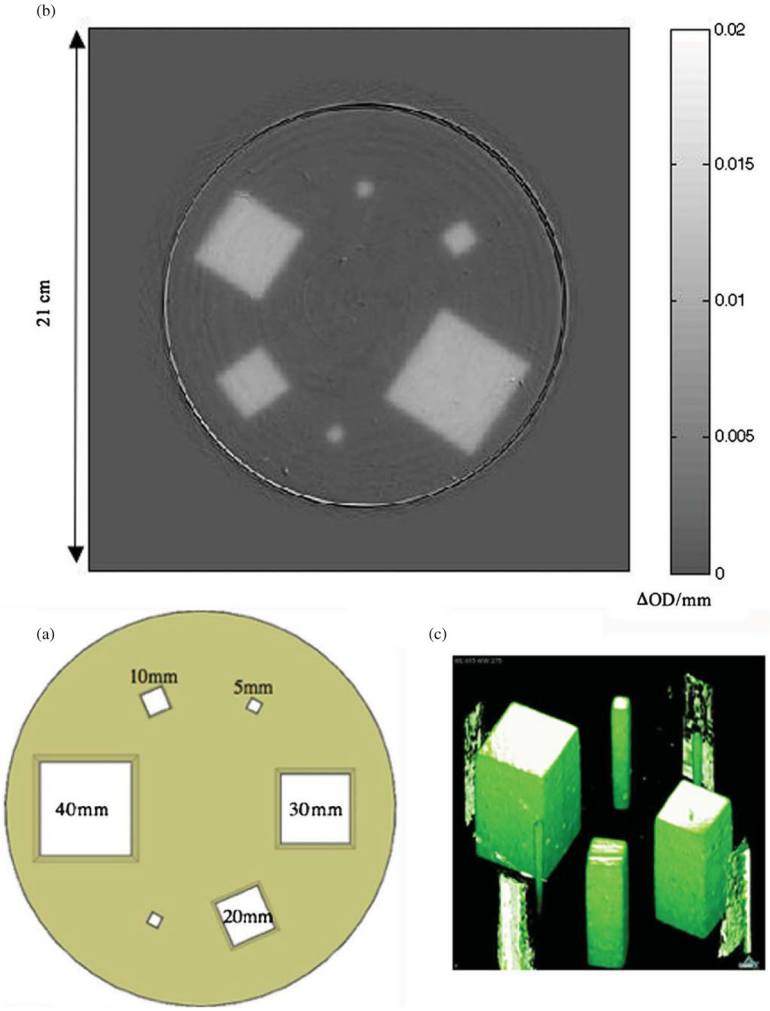

Figure 1.

(a) A beam's eye view of the six photon field irradiation orientation for total scatter factor and profile measurements using a large PRESAGE® dosimeter. The fields were arranged to minimize the scatter dose contamination from one field into another. (b) OCTOPUS optical-CT scan of the PRESAGE® dosimeter. The array is a 0.5 mm thick reconstructed slice at a depth of 5 cm with 0.5 × 0.5 × 0.5 mm voxels. The color scale values indicate radiation-induced change in OD per mm. These values are proportional to absorbed dose. (c) Three-dimensional rendering of the PRESAGE® dosimeter.

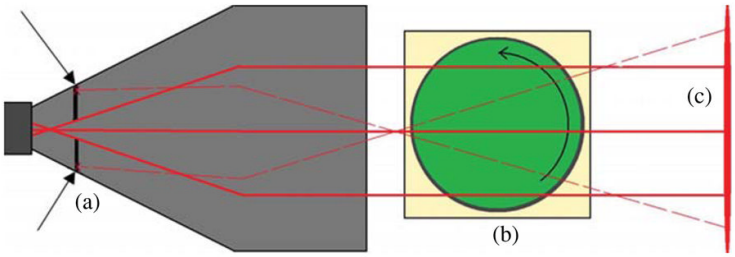

Figure 2.

A top view (not to scale) of the CCD-based optical-CT scanner (54 mm × 72 mm FOV) illustrates the rejection of nonparallel light (dashed lines). A CCD camera and telecentric lens (a) only accepts incoming light rays that are parallel to the optical axis within 0.2°. An aquarium (b) houses refractive index matching fluid, PRESAGE® sample and rotation stage. The sample rotates within the aquarium while multiple projection images are acquired. The refractive index matching fluid limits reflection and refraction of light traversing the sample. The uniform monochromatic backlight (c) emits a narrow band of wavelengths centered on 633 nm.

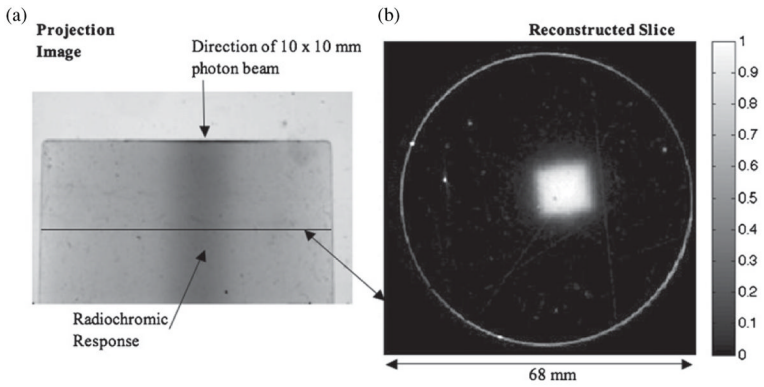

Figure 3.

(a) A projection image of the PRESAGE® sample captured with a prototype CCD-based optical-CT scanner. The radiochromic change produced by the 10 × 10 mm beam is visible (shown by arrow) through the center of the dosimeter. The horizontal line denotes the location of the reconstructed slice (b) through the dosimeter. The pixel values in the reconstructed slice reflect relative absorbed dose. Some of the imperfections in the PRESAGE® are visible in the reconstructed slice and the projection image. This could be a leading source of error in these measurements.

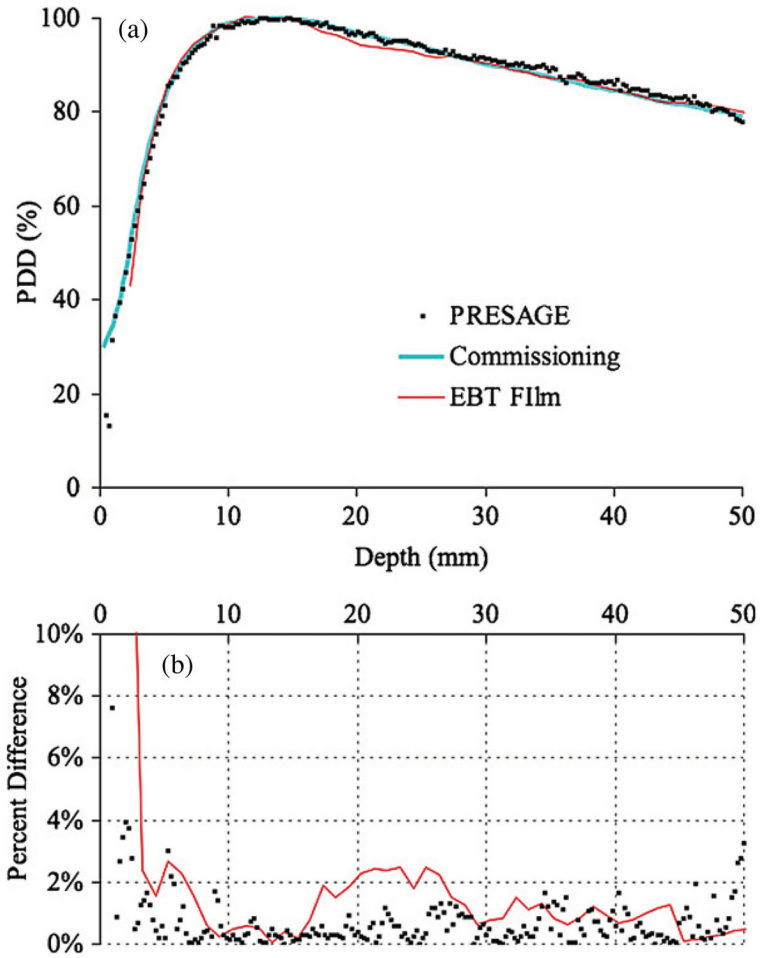

Figure 4.
(a) Percent depth dose measured with a small PRESAGE® dosimeter, EBT film, and with a high-resolution diode during commissioning. The plot shows percent depth dose for 6 MV beam in normal mode (600 MU min^{-1}) with an HDMLC square field size of 10 mm. (b) Percent difference between the three experimental measurement techniques and the commissioning PDD (measured with a high-resolution diode).

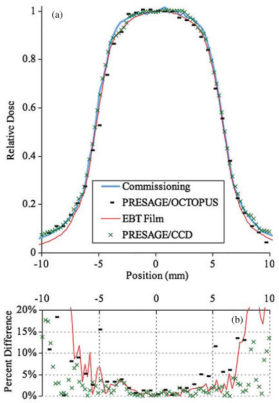

Figure 5.

(a) 10 mm field profile at a depth of 5 cm measured with EBT film, the PRESAGE®/OCTOPUS optical-CT system and a prototype PRESAGE®/CCD optical-CT system. (b) Percent difference between the three experimental measurement techniques and the commissioning profile (measured with a high-resolution diode).

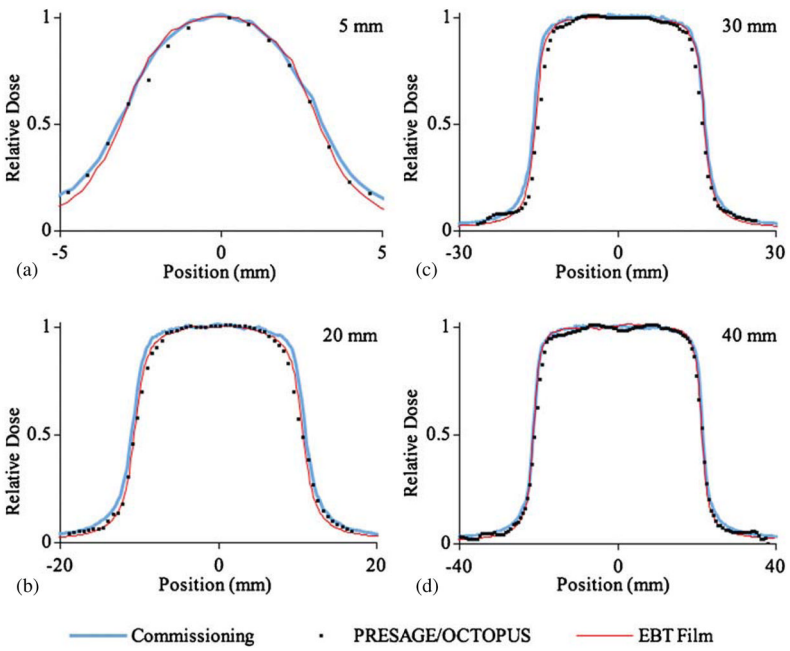

Figure 6.
Profiles at a depth of 5 cm measured with EBT film and PRESAGE®/OCTOPUS optical-CT system. Commissioning measurements are also shown. (a) 5 mm field profile, (b) 20 mm field profile, (c) 30 mm field profile and (d) 40 mm field profile.

Table 1

A summary of the measurements made with Gafchromic EBT® film, the PRESAGE®/OCTOPUS system and a prototype PRESAGE®/CCD optical scanner. During commissioning, output measurements were made for 40, 20, 10 and 5 mm radiosurgery fields (Ionization Chamber CC01, Wellhofer) while profiles and PDDs were measured for 40, 30, 20, 10 and 5 mm fields (Hi-pSi stereotactic field detector, Scanditronix)

	Gafchromic EBT® film	**PRESAGE® (CCD)**	**PRESAGE® (OCTOPUS)**
$S_{c,\,p}$ (30, 20, 10, 5 mm fields)	X		X
PDD (10 mm field)	X	X	
Profile and penumbra (40, 30, 20, 10, 5 mm fields)	X		X
Profile and penumbra (10 mm field)		X	

Table 2

An assessment of the effect of inter-field dose contamination when measuring $S_{c,\,p}$ in the field geometry in figure 1(a). The 'combined geometry' is shown in figure 1(a). The 'separate geometry' refers to the irradiation of one piece of film per field

Field size (mm)	EBT (combined geometry)	EBT (separate geometry)	Percent error
30 × 30	0.901 ± 0.018	0.892 ± 0.018	1.0%
20 × 20	0.899 ± 0.018	0.886 ± 0.018	1.5%
10 × 10	0.802 ± 0.016	0.795 ± 0.016	0.8%
5 × 5	0.642 ± 0.013	0.636 ± 0.013	0.7%

Table 3

Total scatter factors measured with PRESAGE®/OCTOPUS optical-CT system and with EBT film. The uncertainty in each individual measurement is shown following each datum. The far right column shows the percent difference between commissioning values and values measured with PRESAGE®, followed by the percent difference between commissioning values and values measured with Gafchromic EBT® film

Field size (mm)	Commissioning data	PRESAGE®	EBT	Percent differences
30 × 30	–	0.901 ± 0.027	0.892 ± 0.076	
20 × 20	0.858	0.856 ± 0.026	0.886 ± 0.075	0.2%, 3.2%
10 × 10	0.767	0.789 ± 0.024	0.795 ± 0.066	2.8%, 3.6%
5 × 5	0.626	0.649 ± 0.019	0.636 ± 0.054	3.6%, 1.6%

Table 4

80–20% penumbrae at a depth of 5 cm measured with PRESAGE® and EBT Film. Profiles for each field are shown in figures 5(a) and 6

Field size (mm)	Commissioning (mm)	PRESAGE® (OCTOPUS) (mm)	PRESAGE® (CCD) (mm)	EBT (mm)
40 × 40	2.7 ± 0.3	3.0 ± 0.6		2.6 ± 0.2
30 × 30	2.5 ± 0.3	2.4 ± 0.6		2.2 ± 0.2
20 × 20	2.5 ± 0.3	2.5 ± 0.6		2.2 ± 0.2
10 × 10	2.2 ± 0.3	2.5 ± 0.6	2.4 ± 0.2	2.0 ± 0.2
5 × 5	1.9 ± 0.3	2.7 ± 0.7		1.6 ± 0.2